Bled Workshops
in Physics
Vol. 19, No. 2

Proceedings to the 21*st Workshop*
What Comes Beyond . . . *(p. 285)*
Bled, Slovenia, June 23–July 1, 2018

13 The Correspondence Between Fermion Family Members in Spin-charge-family Theory and Structure Defects in Electrically-charged Tessellations

E.G. Dmitrieff *

Irkutsk State University, Russia

Abstract. In this article we compare spinor representations in the the Spin-charge-family theory with the possible charge distributions in spatial tessellations. Particularly, we considered alternations of opposite-charged binary triangles and the Weaire-Phelan structure, and found out that the correspondence between anti-structural defects and representations of fundamental fermions can be established.

Povzetek. Prispevek primerja spinorske upodobitve v teoriji *Spinov-nabojev-družin* z možnimi porazdelitvami naboja v prostorskih teselacijah. Lastnosti alternirajočih binarnih trikotnikov z nasprotnimi naboji v Weaire-Phelanovih strukturah z antistrukturnimi defekti poveže z lastnostmi kvarkov in leptonov.

Keywords: Particle model, Weaire-Phelan tessellation, Spin-charge-family theory

13.1 Introduction

A fermion family derived in spin-charge-family theory [1] consists of 64 members, that differs from each other by their color, weak charge, hyper-charge, electric charge, handedness, and spin.

The theory starts from several assumptions, including metric, action in $13+1$ dimensions, and the schema of symmetry breaks. Also, the theory postulates the basic vacuum state formed by two right-handed neutrinos with opposite spins, and the set of operators, acting on this state, that are members of Clifford algebra.

Each particular fermion state is produced by applying operators

$$S^{ab} = \frac{i}{4}\{\gamma^a, \gamma^b\}_- = \frac{i}{2}\gamma^a\gamma^b \, (a \neq b), \tag{13.1}$$

that are infinitesimal generators of the Lorentz transformations, to the vacuum state.

One can obtain quantum numbers of each state as a combination of eigenvalues $k_{ab}/2$ of these operators,

$$(k_{ab})^2 = \eta^{aa}\eta^{bb}, \tag{13.2}$$

* E-mail: eliadmitrieff@gmail.com

that are ± 1 or $\pm i$ since the metric $\eta^{ab} = diag(-1, 1, 1...1)$:

$$S^{ab}\,(\overset{ab}{k_{ab}}) = \frac{k_{ab}}{2}(\overset{ab}{k_{ab}}), S^{ab}\,[\overset{ab}{k_{ab}}] = \frac{k_{ab}}{2}[\overset{ab}{k_{ab}}]. \tag{13.3}$$

Here

$$\begin{aligned}(\overset{ab}{k_{ab}}) &= \frac{1}{2}\left(\gamma^a + \frac{\eta^{aa}}{ik_{ab}}\gamma^b\right),\\ [\overset{ab}{k_{ab}}] &= \frac{1}{2}\left(I + \frac{i}{k_{ab}}\gamma^a\gamma^b\right)\end{aligned} \tag{13.4}$$

and γ^a, γ^b are the Clifford algebra objects following the defining equation

$$\left\{\gamma^a;\gamma^b\right\}_+ = 2\eta^{ab}I \tag{13.5}$$

with the metric $\eta^{ab} = diag(-+++\cdots+)$ and unit matrix I.

We found out that these k_{ab} can be mapped to the structure close to the Weaire-Phelan tessellation [4], assuming its cells carrying electric charge of $\pm\frac{1}{6}e$ [5], [3].

We recognize it as a possible mechanism for manifestation of the 13+1-dimensional spin-charge-family theory in the 3-dimensional space.

13.2 Charged binary triangles

We consider the small model system containing three unordered elements having the electrical charge of either $+\frac{1}{6}e$ or $-\frac{1}{6}e$[1]. Since the elements are unordered, one can imagine this system as an equilateral triangle with elements residing in its vertices (Fig. 13.1A). The system has three binary degrees of freedom and possesses $SU(3)$ symmetry of its possible states.

13.2.1 Charged binary triangle's state space

The state space of charged binary triangles, shown on Fig. 13.1B, contains $2^3 = 8$ states. In three-dimensional Cartesian reference frame with its axes representing states of particular elements, it looks like a cube.

One of these eight states has the total electric charge $q = 3 \times (-\frac{1}{6}) = -\frac{1}{2}$, three states have $q = -\frac{1}{6}$, another three states have $q = +\frac{1}{6}$, and, again, one has $q = +\frac{1}{2}$. These counts are binomial coefficients for $n = 3$ and the charge values coincide with eigenvalues of τ^4, that is the $U(1)$ *fermion charge* operator in the spin-charge-family theory:

$$\tau^4 = -\frac{1}{3}\left(S^{9\,10} + S^{11\,12} + S^{13\,14}\right) = -\frac{1}{6}\left(k_{9\,10} + k_{11\,12} + k_{13\,14}\right). \tag{13.6}$$

One can see that among four diagonals of this cube there are three diagonals of one kind, connecting states with difference of $\frac{1}{6}$, and one of another kind,

[1] Further we omit the e unit

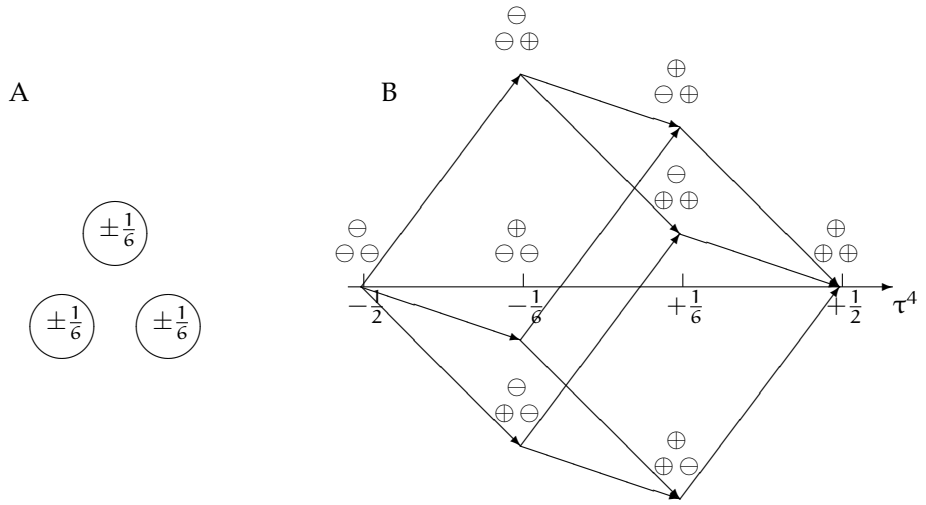

Fig. 13.1. (A) The system of three elements charged with $\pm\frac{1}{6}e$ and (B) its three-dimensional state space containing eight possible states

connecting states with the difference of 1. This dedicated "main" diagonal is the τ^4 axis since the projections of cube vertex on it coincide with τ^4 eigenvalues.

The edge of the state cube is therefore $\frac{1}{\sqrt{3}}$, and the radius from τ^4 axis to non-axial states is $r = \frac{\sqrt{2}}{3}$.

Consider the isometric projection of the state cube onto Cartesian coordinate plain that is orthogonal to the τ^4 axis (Fig. 13.2). Let the ordinate axis to be directed opposite to the edge corresponding to $k_{13\,14}$. Then the projections of states on the abscissas and ordinate axes, divided by projection distortion of $\sqrt{\frac{2}{3}}$, coincide with *color charge* components τ^{33} and τ^{38}, respectively:

$$\begin{aligned}
\tau^{33} &= \frac{1}{2}\left(S^{9\,10} - S^{11\,12}\right) = \frac{1}{4}\left(k^{9\,10} - k^{11\,12}\right) = \\
&= \frac{\sqrt{2}}{3}\cos\left(\frac{\pi}{6} + \frac{\pi n}{6}\right) \times \sqrt{\frac{3}{2}} \in \left\{0; \pm\frac{1}{2}\right\}, \\
\tau^{38} &= \frac{1}{2\sqrt{3}}\left(S^{9\,10} + S^{11\,12} - S^{13\,14}\right) = \frac{1}{4\sqrt{3}}\left(k^{9\,10} + k^{11\,12} - k^{13\,14}\right) = \\
&= \frac{\sqrt{2}}{3}\sin\left(\frac{\pi}{6} + \frac{\pi n}{6}\right) \times \sqrt{\frac{3}{2}} \in \left\{\pm\frac{1}{\sqrt{3}}; \pm\frac{1}{2\sqrt{3}}\right\}.
\end{aligned} \tag{13.7}$$

13.2.2 Model with alternation of charged binary triangles

Note that a charged binary triangle cannot be electrically neutral. Nevertheless, a pair of opposite-charged binary triangles, or, generally, any even number of them can hold zero electric charge.

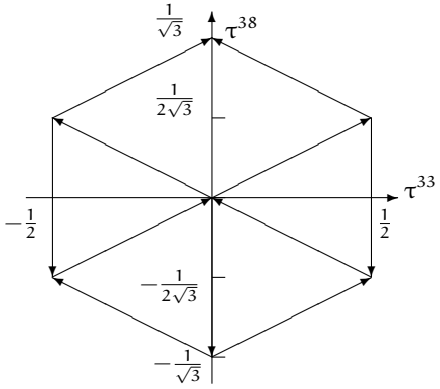

Fig. 13.2. The isometric projection of the state cube along the τ^4 axis

Consider a big system containing sufficiently large amount of opposite-charged binary triangles, half of them consisting of three positive-charged elements, and half of three negative-charged ones, arranged in alternating pattern. The whole system is electrically neutral.

Each triangle in this system, either having charge of $+\frac{1}{2}$ or $-\frac{1}{2}$, is surrounded by opposite-charged environment with the same magnitude:

$$q_{env} = -\tau^4. \tag{13.8}$$

We found out that in this system, where positive- and negative-charged triangles have different *own* places due to their alternation, the additional degree of freedom emerges for any single triangle.

For instance, the negative-charged triangle with $q = \tau^4 = -\frac{1}{2}$ in its own place must be effectively neutralized by its environment and therefore must be indistinguishable from the background. But the same triangle in the place of positive-charged one should be treated as having effective charge of -1 that emerges as a sum of the negative triangle charge and the negative charge of the environment surrounding the place where the positive triangle should be:

$$Q = \tau^4 + q_{env} = -\frac{1}{2} + \left(-\frac{1}{2}\right) = -1. \tag{13.9}$$

So the state space for the charged binary triangle that participates in the neutral alternation of such triangles, must reflect this emergent binary degree of freedom. The state space becomes four-dimensional, splitting each original state to the doublet with the triple magnitude $\frac{1}{2}$ in comparison to original $\frac{1}{6}$ (Fig. 13.3). One of the states shifts *up* in charge with $+\frac{1}{2}$ while another one shifts *down*, with $-\frac{1}{2}$.

One can ensure that among these 16 states there are neutral and integer- and fractional-charged ones with step of $\frac{1}{3}$ so the effective charges coincide with charges of known fundamental fermions and anti-fermions belonging to one family.

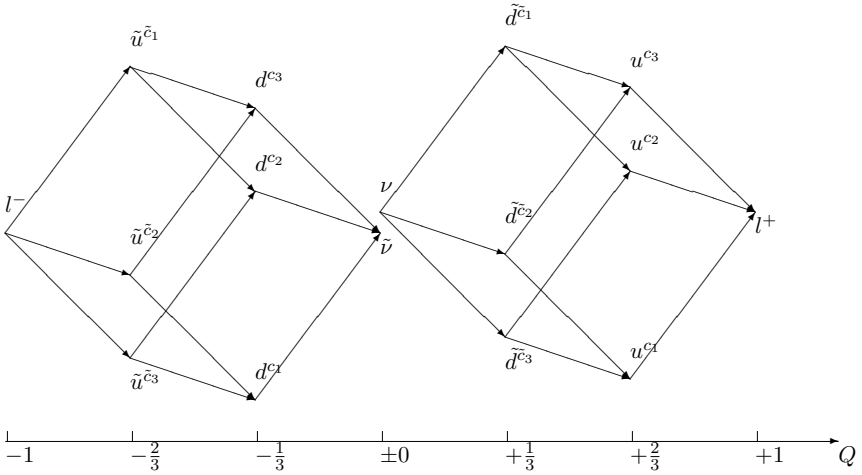

Fig. 13.3. Four-dimensional state hyper-rectangle space for the single charged binary triangle in the environment of neutral tessellation of alternating $\pm\frac{1}{2}$-charged binary triangles, labeled with symbols of corresponding fermion family members

The degree of freedom emerging from implementing the tessellation instead of isolated triangle manifests the physical sense of the *isospin*, or the *weak charge*, connecting corresponding up and down particles.

Following the observations mentioned above, we suppose that one should search for geometrical structure containing equilateral triangles, aiming to obtain suitable model for the fundamental particles. It must be chiral to represent handedness and also must possess some additional degrees of freedom to be able to represent fermion families and fundamental bosons.

13.3 Calculation of electrical charge and Weaire-Phelan tessellation

We consider a graph for calculating the electric charge Q from values k_{ab} [1], that are the doubled eigenvalues (13.3) of Lorentz transformations infinitesimal generators S^{ab} (13.1) [1], [2]. The graph is constructed aiming to fetch all the data required for the calculation from the charges of cells in the dual-charged Weaire-Phelan tessellation [5].

In the Spin-Charge-Family theory, as well as in the Standard Model, the electric charge of a particle is calculated as a sum of the third projection of its $SU(2)_I$ weak charge τ^{13} and the hypercharge Y:

$$Q = \tau^{13} + Y. \tag{13.10}$$

Since the weak charge operator is defined as

$$\vec{\tau}^1 = \frac{1}{2}\left(S^{58} - S^{67}, S^{57} + S^{68}, S^{56} - S^{78}\right), \tag{13.11}$$

and each S^{ab} has two eigenvalues, namely $\frac{1}{2}k_{ab}$, where $k_{ab} = \pm 1$, the weak charge is expressed through k_{ab} in the following way:

$$\tau^{13} = \frac{1}{4}k_{56} - \frac{1}{4}k_{78}. \tag{13.12}$$

Therefore it can be of one of three different values:

k_{56}	k_{78}	τ^{13}
-1	-1	0
1	1	0
-1	1	$-1/2$
1	-1	$1/2$

In turn, the hypercharge is the sum of $SU(2)_{II}$ charge τ^{23} and $U(1)$ "fermion charge" τ^4:

$$Y = \tau^{23} + \tau^4, \tag{13.13}$$

where

$$\vec{\tau}^2 = \frac{1}{2}\left(S^{58} + S^{67}, S^{57} - S^{68}, S^{56} + S^{78}\right) \tag{13.14}$$

and

$$\tau^4 = -\frac{1}{3}\left(S^{9\,10} + S^{11\,12} + S^{13\,14}\right). \tag{13.15}$$

After transition to the eigenvalues,

$$\tau^{23} = \frac{1}{4}k_{56} + \frac{1}{4}k_{78}, \tag{13.16}$$

$$\tau^4 = -\frac{1}{6}k_{9\,10} - \frac{1}{6}k_{11\,12} - \frac{1}{6}k_{13\,14}. \tag{13.17}$$

So

$$Y = \frac{1}{4}k_{56} + \frac{1}{4}k_{78} - \frac{1}{6}k_{9\,10} - \frac{1}{6}k_{11\,12} - \frac{1}{6}k_{13\,14}, \tag{13.18}$$

and, finally,

$$Q = \frac{1}{4}k_{56} - \frac{1}{4}k_{78} + \frac{1}{4}k_{56} + \frac{1}{4}k_{78} - \frac{1}{6}k_{9\,10} - \frac{1}{6}k_{11\,12} - \frac{1}{6}k_{13\,14}. \tag{13.19}$$

One can build the following graph illustrating how the electrical charge is calculated, where the arcs show the data dependence between nodes:

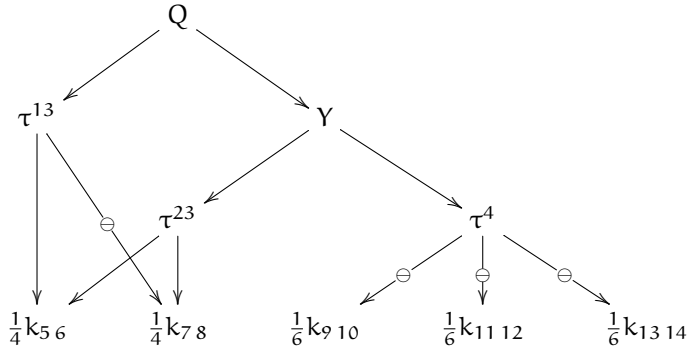

The value of k_{78} is included in equation (13.19) twice, with opposite signs, so it has no influence on the total charge Q, and the equation can be *simplified*:

$$Q = \frac{1}{2}k_{56} - \frac{1}{6}k_{9\,10} - \frac{1}{6}k_{11\,12} - \frac{1}{6}k_{13\,14}. \tag{13.20}$$

The corresponding simplified calculation graph is the following:

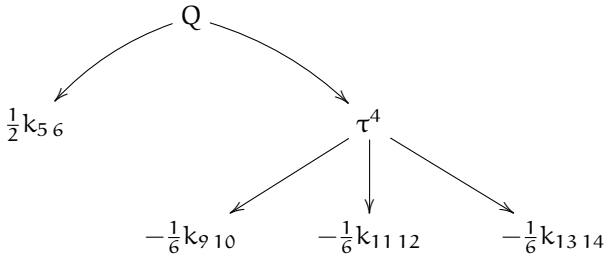

In this form, the graph is equivalent to the charge calculation in our 4-bit model presented in [3]:

$$Q = \sum_{i=0}^{2} \frac{c_i}{3} - q_2, \tag{13.21}$$

with the following correspondence:

$$\begin{aligned}
&\frac{1}{2}k_{56} = -(q_2 - \frac{1}{2})\\
&\frac{1}{6}k_{9\,10} = -\frac{1}{3}(c_0 - \frac{1}{2})\\
&\frac{1}{6}k_{11\,12} = -\frac{1}{3}(c_1 - \frac{1}{2})\\
&\frac{1}{6}k_{13\,14} = -\frac{1}{3}(c_2 - \frac{1}{2}).
\end{aligned} \tag{13.22}$$

The $c_i \in \{0;1\}$ are three bits of the color code and $q_2 \in \{0;1\}$ is the most significant bit of the electrical charge code in the *ones' complement* convention.

After splitting the node $\frac{1}{2}k_{5\,6}$ into three nodes $\frac{1}{6}k_{5\,6}^{(1)}$, $\frac{1}{6}k_{5\,6}^{(2)}$, and $\frac{1}{6}k_{5\,6}^{(3)}$, the graph becomes equivalent to our 6-bit model [3]:

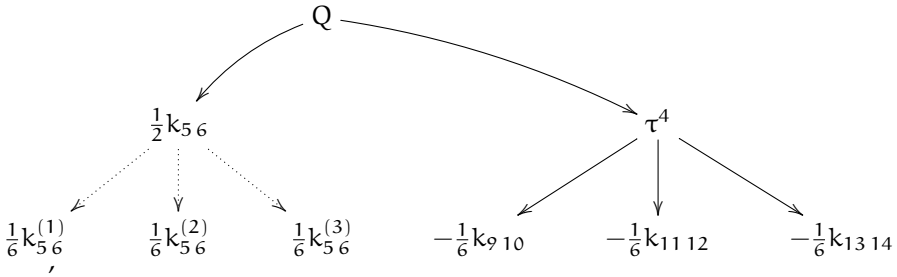

$$Q = \sum_{i=0}^{2} b_i^c + \sum_{i=0}^{2} b_i^{T_3}, \tag{13.23}$$

where symbols b_i^c are produced from c_i by scaling and shifting down:

$$b_i^c = \frac{c_i}{3} - \frac{1}{6}, i \in \{0;1;2\}; b_i^c \in \left\{-\frac{1}{6}; \frac{1}{6}\right\}. \tag{13.24}$$

The symbols $b_i^{T_3}$ are produced from q_2 by splitting it into three parts, scaling and shifting up:

$$b_i^{T_3} = \frac{1}{6} - \frac{q_2}{3}, i \in \{0;1;2\}, b_i^{T_3} \in \left\{-\frac{1}{6};\frac{1}{6}\right\} \tag{13.25}$$

Note that we do not mean an increase in the number of degrees of freedom as a consequence of splitting nodes, at least while considering members of one fermion family, since all the three subnodes are assumed keeping the same values that are equal to value of splitted node..

Both these graphs have the following advantage in relation to the original one: they allow interpretation of particle's electrical charge as a *simple sum of values of all the nodes*[2] due to its tree-form and arcs meaning addition only. The last one also has an advantage of equal magnitude of nodes[3].

To get these advantages in the original graph, we transform it the following way, getting rid of two loops and the subtracting arc. To do so, we assume that there are two *different* subnodes behind $\frac{1}{4}k_{5\,6}$ and two others behind $\frac{1}{4}k_{7\,8}$, always keeping *equal* values in the first case, and *opposite* values in the second one.

After transformation the graph becomes the following:

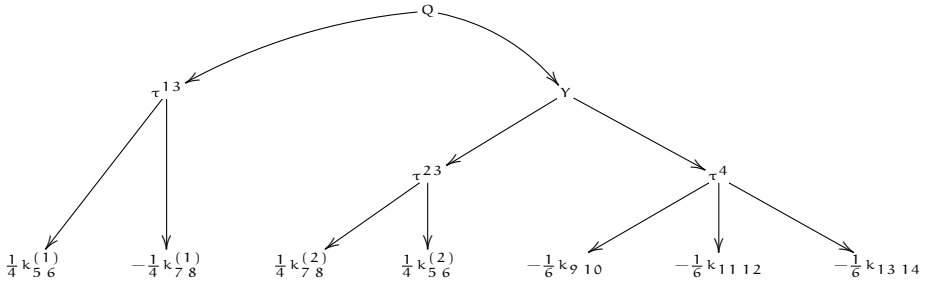

Then we double the factors in all the nodes for $k_{5\,6}$ and $k_{7\,8}$, introducing compensating nodes that divide the corresponding values back. That makes these nodes ready to split on three sub-nodes with the factor of $\frac{1}{6}$. Arguments in favor of division in half for nodes $k_{5\,6}$ and $k_{7\,8}$ are different and given below and are discussed in detail in [5].

[2] or integration of charge density in continuous models

[3] The choice of positive or negative eigenvalues is made while choosing the initial vacuum state corresponding to the right neutrino, and it can be changed to eliminate minus signs.

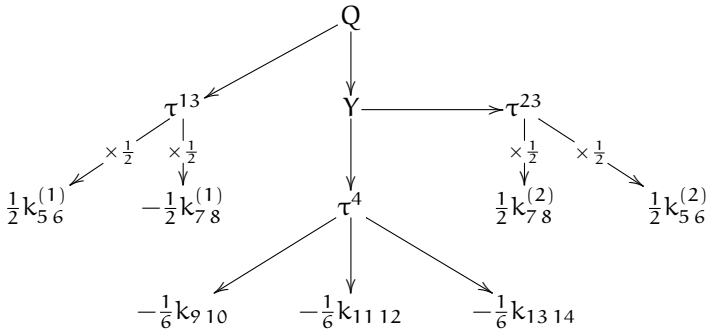

At the last step, we split each node $k_{5\,6}$, $k_{7\,8}$ to three sub-nodes. Then we establish correspondence between these nodes and cells in the dual-charged Weaire-Phelan tessellation:

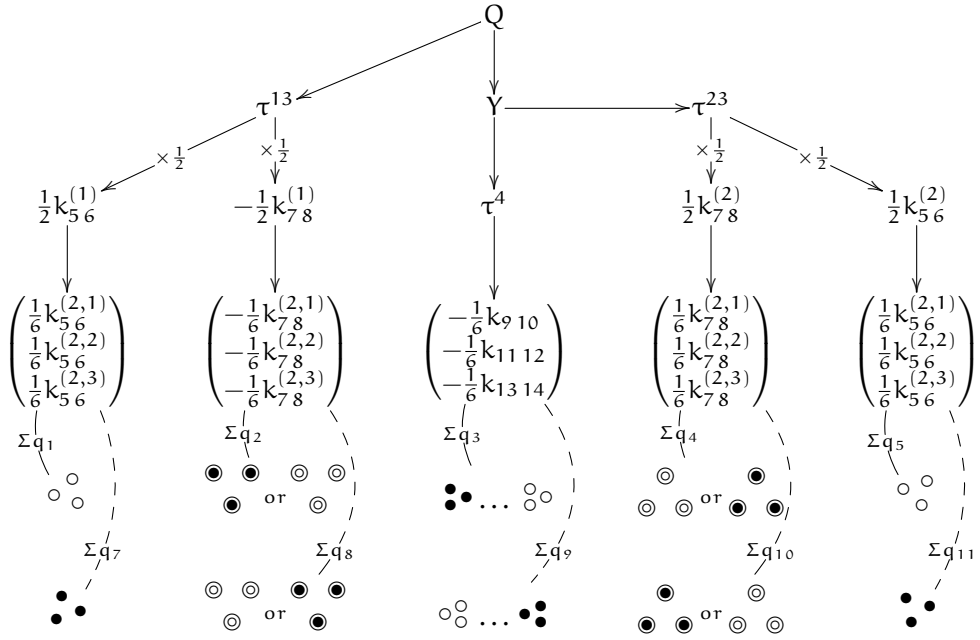

The last two rows contain the corresponding triangles of charged cells, residing in sequential ζ-planes in the tessellation. These triangles are listed in the Table 13.1 (it is borrowed from [5]). The first row contains cells triangles in planes from 1 to 5 and represents down fermions; in turn, the charge-inversed and mirror-reflected triangles in planes from 7 to 11 represent corresponding up particles.

Note that cells in planes 1 and 5, 7 and 11, that are the data sources for the $k_{5\,6}$ nodes, do not have any degrees of freedom and carry the negative charge for down particles and positive for up particles. Since all six cells are equal in charge and they must represent the $q_{env} = \pm\frac{1}{2}$, i.e. charge of the *environment* for cells in planes 3 or 9, their charge value is divided in half.

$\zeta, \times \frac{1}{\sqrt{3}}$	kind, charge	shape	size	shape description
0	D−	◎	−	Axial D−
1	T−	○ ○ ○ ◉ ◉	$\sqrt{14}$	Large T− triangle counterclockwise
2	D+	◉	$\sqrt{32}$	D+ triangle υ-down
3	T+	● ●	$\sqrt{6}$	Small T+triangle (ξ-right)
4	D−	◎ ◎ ◎	$\sqrt{32}$	D− triangle υ-up
5	T−	○ ○	$\sqrt{14}$	Large T− triangle clockwise
6	D+	◉	−	Axial D+
7	T+	● ● ◎ ◎	$\sqrt{14}$	Large T+ triangle clockwise
8	D−	◎	$\sqrt{32}$	D− triangle υ-down
9	T−	○ ○	$\sqrt{6}$	Small T− triangle (ξ-left)
10	D+	◉ ◉ ◉	$\sqrt{32}$	D+ triangle υ-up
11	T+	● ●	$\sqrt{14}$	Large T+ triangle counterclockwise
12	D−	◎	−	Axial D−

Table 13.1. Shapes of cell center placements in twelve different planes

The cells in planes 2 and 4, 8 and 10 provide the data for the $k_{7\,8}$ nodes and each couple of triplets has just one degree of freedom, that represent the exchange between triangles in the coupled plane. The exchanged electrical charge of $\frac{1}{2}$ moves from one side of the plane 3 or 9 to another, representing the change of handedness and adjustment of weak charge and hyper-charge.

Since the cells in planes 2 and 4, 8 and 10 appear to have finite size, they partially overlap in projection to $zeta$ axis, providing only *half* of charge is exchanged.

The three cells in plane 3, and three cells in plane 9 provide data for $k_{9\,10}$, $k_{11\,12}$, and $k_{13\,14}$. Each of them keeps its degree of freedom, so there are eight combinations for small triangle in these planes, corresponding to eight down- and eight up particles or antiparticles.They are listed in Tables 13.2 and 13.3.

Note that in our approach the corresponding down and up particles with the same color have in this representation the *opposite* projections to the τ^{38} axis. It is so because they are mirror reflections of each other due to the **P** operation between them (C operation is not applied because we list all 8 combinations of charge for both cases, q_3 and q_9, in the same order). The spin-charge-family theory, in contrast, provides *equal* τ^{38} values in this case [2].

13.3.1 On k numbers without influence on total electric charge

The value of $k_{7\,8}$ has no contribution to the total electric charge. As we have shown above, it can be considered as existing of mutually compensating cells of opposite charges. Also we note that the expression (13.19) can be *expanded* by including

$\tau^{13} =$ $q_{1,2}$	q_3^{210}	q_3^{102}	q_3^{021}	$\tau^4 =$ Σq_3	$\tau^{23} =$ $q_{4,5}$	$Y =$ $q_{3,4,5}$	$Q =$ $\tau^{13} + Y$	sym-bol	$\tau^{33} = \Sigma q_{3\upsilon} \times\sqrt{\frac{3}{2}}$	$\tau^{38} = \Sigma q_{3\xi} \times\sqrt{\frac{3}{2}}$
	+	+	+	+1/2		0	0	$\tilde{\nu}_L$	0	0
	−	+	+					d_R^{c1}	0	$-\frac{1}{\sqrt{3}}$
	+	−	+	+1/6		−1/3	−1/3	d_R^{c2}	+1/2	$\frac{1}{2\sqrt{3}}$
$\frac{1}{2}\times$	+	+	−		$\frac{1}{2}\times$			d_R^{c3}	−1/2	$\frac{1}{2\sqrt{3}}$
	+	−	−					$\tilde{u}_L^{\bar{c}1}$	0	$\frac{1}{\sqrt{3}}$
0	−	+	−	−1/6	−1/2	−2/3	−2/3	$\tilde{u}_L^{\bar{c}2}$	−1/2	$-\frac{1}{2\sqrt{3}}$
	−	−	+					$\tilde{u}_L^{\bar{c}3}$	+1/2	$-\frac{1}{2\sqrt{3}}$
	−	−	−	−1/2		−1	−1	l_R^-	0	0
	+	+	+	+1/2		+1/2	0	$\tilde{\nu}_R$	0	0
	−	+	+					d_L^{c1}	0	$-\frac{1}{\sqrt{3}}$
	+	−	+	+1/6		+1/6	−1/3	d_L^{c2}	+1/2	$\frac{1}{2\sqrt{3}}$
$\frac{1}{2}\times$	+	+	−		$\frac{1}{2}\times$			d_L^{c3}	−1/2	$\frac{1}{2\sqrt{3}}$
	+	−	−					$\tilde{u}_R^{\bar{c}1}$	0	$\frac{1}{\sqrt{3}}$
−1/2	−	+	−	−1/6	0	−1/6	−2/3	$\tilde{u}_R^{\bar{c}2}$	−1/2	$-\frac{1}{2\sqrt{3}}$
	−	−	+					$\tilde{u}_R^{\bar{c}3}$	+1/2	$-\frac{1}{2\sqrt{3}}$
	−	−	−	−1/2		−1/2	−1	l_L^-	0	0

Table 13.2. Eight cases of inversions in the small T-triangle at $\zeta = 3/\sqrt{3}$; with original and exchanged D-triangles at $\zeta = 2/\sqrt{3}$ and $4/\sqrt{3}$, associated with "down" fermions

$\tau^{13}=\Sigma q_{7,8}$	q_9^{234}	q_9^{423}	q_9^{342}	$\tau^4=\Sigma q_9$	$\tau^{23}=\Sigma q_{10,11}$	$Y=\Sigma q_{9,10,11}$	$Q=\tau^{13}+Y$	symbol	$\tau^{33}=\Sigma q_{9\upsilon}$ $\times\sqrt{\frac{3}{2}}$	$\tau^{33}=\Sigma q_{9\xi}$ $\times\sqrt{\frac{3}{2}}$
	+	+	+	+1/2		+1	+1	ι_L^+	0	0
	−	+	+					$u_R^{c\,1}$	0	$\frac{1}{\sqrt{3}}$
	+	−	+	+1/6		+2/3	+2/3	$u_R^{c\,2}$	+1/2	$-\frac{1}{2\sqrt{3}}$
$\frac{1}{2}\times$	+	+	−		$\frac{1}{2}\times$			$u_R^{c\,3}$	−1/2	$-\frac{1}{2\sqrt{3}}$
	+	−	−					$\check{d}_L^{\bar{c}\,1}$	0	$-\frac{1}{\sqrt{3}}$
0	−	+	−	−1/6	+1/2	+1/3	+1/3	$\check{d}_L^{\bar{c}\,2}$	−1/2	$\frac{1}{2\sqrt{3}}$
	−	−	+					$\check{d}_L^{\bar{c}\,3}$	+1/2	$\frac{1}{2\sqrt{3}}$
	−	−	−	−1/2		0	0	$\boxed{\nu_R}$	0	0
	+	+	+	+1/2		+1/2	+1	ι_R^+	0	0
	−	+	+					$u_L^{c\,1}$	0	$\frac{1}{\sqrt{3}}$
	+	−	+	+1/6		+1/6	+2/3	$u_L^{c\,2}$	+1/2	$-\frac{1}{2\sqrt{3}}$
$\frac{1}{2}\times$	+	+	−		$\frac{1}{2}\times$			$u_L^{c\,3}$	−1/2	$-\frac{1}{2\sqrt{3}}$
	+	−	−					$\check{d}_R^{\bar{c}\,1}$	0	$-\frac{1}{\sqrt{3}}$
+1/2	−	+	−	−1/6	0	−1/6	+1/3	$\check{d}_R^{\bar{c}\,2}$	−1/2	$\frac{1}{2\sqrt{3}}$
	−	−	+					$\check{d}_R^{\bar{c}\,3}$	+1/2	$\frac{1}{2\sqrt{3}}$
	−	−	−	−1/2		−1/2	0	ν_L	0	0

Table 13.3. Eight cases of inversions in the small T-triangle at $\zeta = 9/\sqrt{3}$, repeated twice with original and exchanged D-triangles at $\zeta = 8/\sqrt{3}$ and $10/\sqrt{3}$, associated with "up" fermions

additional terms, arbitrary in magnitude, that cancel each other. Since they have no influence on the electrical charge, they can't be determined from the charge analyse. We suppose that the expression of the electrical charge can also contain the last real eigenvalue, $k_{1\,2}$:

$$Q = a k_{12}^{(1)} - a k_{12}^{(2)} + \frac{1}{4} k_{56} - \frac{1}{4} k_{78} + \frac{1}{4} k_{56} + \frac{1}{4} k_{78} - \frac{1}{6} k_{9\,10} - \frac{1}{6} k_{11\,12} - \frac{1}{6} k_{13\,14}, \quad (13.26)$$

where a is a factor that can be equal to $1/6$. It allows to associate $k_{12}^{(1)}$, $k_{12}^{(2)}$ with the "axial" D cells at $\zeta = 0$ and $6/\sqrt{3}$ for down fermions, and $6/\sqrt{3}$ and $12/\sqrt{3}$ for up ones.

In the spin-charge theory the value of k_{03} is dependent on values of other k_{ab} since the equation

$$k_{03} = -i k_{12} k_{56} k_{78} k_{9\,10} k_{11\,12} k_{13\,14} \quad (13.27)$$

is fulfilled for each fermion combination in [1], [2]. In our opinion, it is connected with the fact that the seven binary values of k_{ab} generate only $2^6 = 64$ combinations. For one family there are only six independent degrees of freedom represented by k_{ab}, so since there are seven of them, one (in our case, k_{03}) should be expressed through six others.

Thus, there is no degree of freedom connected with k_{03} and there is no corresponding cell in the Weaire-Phelan structure, so the value of *spin* always can be computed based on other data 13.27.

Totally, we have the following correspondence between values of k_{ab} in the Spin-Charge-Family theory and charges associated with cells of dual-charged Weaire-Phelan model:

$$\begin{aligned}
k_{1\,2} &= 3q_{-3} - 3q_{+3} \\
k_{5\,6} &= \Sigma q_{-2} + \Sigma q_{+2} \\
k_{7\,8} &= \Sigma q_{-1} - \Sigma q_{+1} \\
k_{9\,10} &= 6q^{ijk} \\
k_{11\,12} &= 6q^{jki} \\
k_{13\,14} &= 6q^{kij} \\
k_{0\,3} &= -i k_{12} k_{56} k_{78} k_{9\,10} k_{11\,12} k_{13\,14}
\end{aligned} \quad (13.28)$$

It is provided in relative form, for both up and down particles. The lower index counting the ζ-plane number relative to the plane of the small T-triangle (that is 3 for down or 9 for up fermions), and the upper index counts x,y,z coordinates of three individual cells in the triangle; the Σ sign means sum of these three cells.

13.4 Conclusion

We presented here our approach to the particle and vacuum modelling. It is, being applied to one fermion family, reproduces the same quantum numbers as those obtained in the spin-charge-family theory. The advantage of spatial tessellation model, on our opinion, is the lower dimension count, so it can fit in the usual

spacetime and be more demonstrative. Also it provides native **CPS** symmetry and emergent weak charge. We suppose that one can find out the appropriate 3- or 4-dimensional spatial model that would, keeping the shown advantages, also represent and explain fermion families and also fundamental bosons, basing on 8-bit code model [3].

References

1. N.S. Mankoč Borštnik: Can spin-charge-family theory explain baryon number non conservation? arXiv:1409.7791v3 - 24 February 2015.
2. N.S. Mankoč Borštnik: Fermions and Bosons in the Expanding Universe by the Spin-charge-family theory, in: N.S. Mankoč Borštnik, H.B.F. Nielsen, D. Lukman: Proceedings to the 20th Workshop 'What Comes Beyond the Standard Models', Bled, July 9 - 17 2017.
3. E.G. Dmitrieff: Experience in modeling properties of fundamental particles using binary codes, in: N.S. Mankoč Borštnik, H.B.F. Nielsen, D. Lukman: Proceedings to the 19th Workshop 'What Comes Beyond the Standard Models', Bled, 11. - 19. July 2016.
4. D.Weaire, R.Phelan, A counter-example to Kelvin's conjecture on minimal surfaces, Phil. Mag. Lett., (1994) 69: 107–110, doi:10.1080/09500839408241577
5. E.G.Dmitrieff: On triple-periodic electrical charge distribution as a model of physical vacuum and fundamental particles, in N.S. Mankoč Borštnik, H.B.F. Nielsen, D. Lukman: Proceedings to the 21th Workshop 'What Comes Beyond the Standard Models', Bled, 23. - 29. June 2018